ISA Transactions 49 (2010) 222–228

Contents lists available at ScienceDirect

ISA Transactions

journal homepage: www.elsevier.com/locate/isatrans

Compact H_∞ robust rebalance loop controller design for a micromachined electrostatically suspended gyroscope

Gaoyin Ma[a,b], Wenyuan Chen[a,*], Weiping Zhang[a,*], Feng Cui[a], Kai Li[a]

[a] National Key Laboratory of Nano/Micro Fabrication Technology, Key Laboratory for Thin Film and Microfabrication of Ministry of Education, Institute of Micro and Nano Science and Technology, Shanghai Jiao Tong University, Shanghai, 200240, China

[b] No. 9 Academy, China Aerospace Science and Technology Corporation, Beijing, 100854, China

ARTICLE INFO

Article history:
Received 21 June 2009
Accepted 11 November 2009
Available online 3 December 2009

Keywords:
Microelectromechanical systems (MEMS)
Gyro
Rebalance loop
H_∞ robust control
Mixed-sensitivity optimization

ABSTRACT

In this paper, we design a compact H_∞ robust rebalance loop controller that is featured with comprehensive performance achievement and relatively easy practical implementation for a dual-axis micromachined rotational gyro. By incorporating the bilinear pole-shifting transform into the weighted multivariable mixed-sensitivity framework, the design procedure of the robust controller is able to allow for various realistic performance requirements in terms of steady-state error, dynamic response characteristics, disturbance rejection and robustness to parametric variations. In comparison with a conventional decentralized lead–lag controller, the H_∞ robust controller, which is considered as an efficient substitute for the former, is thoroughly analyzed and simulationally validated under a set of realistic scenarios.

1. Introduction

A rotational microelectromechanical system (MEMS) gyro usually consists of a spinning suspended rotor in a vacuum cavity and several sets of electrodes that are symmetrically arranged on the inner surface of the cavity. As a sensing element, the rotor is electrostatically suspended in its null position by means of multi-axis closed-loop control systems, and spins at a preselected speed on the principle of a variable capacitance micromotor [1–4]. In this way, the rotational MEMS gyro can eliminate undesirable mechanical friction and achieve higher sensitivity in comparison with a vibratory MEMS gyro [5]. Furthermore, the rotational MEMS gyro can simultaneously detect dual-axis angular rate inputs that are orthogonal to the spinning axis with potential high resolution. Therefore, gyros of this kind have important prospective applications such as Micro Aerial Vehicles (MAVs), advanced automotive safety systems and microrobotics.

Such a gyro is designed and fabricated by our research group, and a slanting exploded view of its schematic structure is shown in Fig. 1(a), and a chip (fixed on a printed circuit board) photograph is depicted in Fig. 1(b). Briefly, it is a vertical sandwich structure and has two stator layers with identical patterns. The radial suspension electrodes are responsible for rotor translation control along the in-plane axes, and the axial suspension electrodes serve to control the rotor's out-of-plane translation and tilts about the in-plane axes. Spinning torques for the suspended rotor are generated from active capacitances between the rotation electrodes and the rotor poles. The main geometrical parameters of the gyro are listed in Table 1 [6].

For the rotational MEMS gyro applied for a strapdown system, a dual-axial rebalance loop is of importance in determining its dynamic range, sensitivity and accuracy. The rebalance loop is mainly composed of capacitive sensing electronics, a controller and electrostatic torquers. When external angular rates about the in-plane axes are applied to a moving vehicle where the gyro case is attached, tilt angles appear between the rotor spinning axis and the gyro case. The tilt angles are detected promptly by the capacitive sensing electronics and then nulled quickly by the electrostatic torquers which rebalance the rotor back to its null position. This dual-axis tilting-rebalance process is dictated essentially by the controller, which plays a substantial role in the whole rebalance loop and is also the subject of this work.

The tilting-rebalance process is largely similar to a coupled two-input–two-output (TITO) industrial process, for which various controllers have been designed by many works [7–10]. Unfortunately, most of them are decentralized designs with classical single-input–single-output (SISO) control theory and cannot provide adequate design freedom and effective robust synthesis and analysis methods that are particularly required in this case [11]. Although

---

[*] Corresponding address: Room 2-301, Research Institute of Micro and Nano Science and Technology, Shanghai Jiao Tong University, 800#, Dongchuan Road, Shanghai, 200240, China. Tel.: +86 21 34206667.

E-mail addresses: chenwy@mail.sjtu.edu.cn (W. Chen), zwp37@163.com (W. Zhang).

0019-0578/$ – see front matter © 2009 ISA. Published by Elsevier Ltd. All rights reserved.
doi:10.1016/j.isatra.2009.11.003

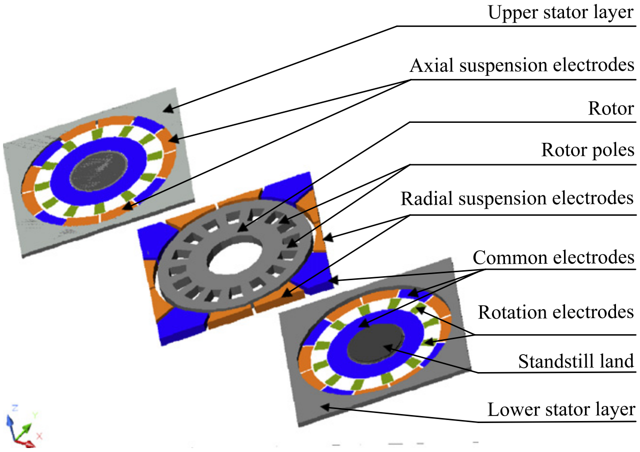

Fig. 1(a). Slanting exploded view of the gyro.

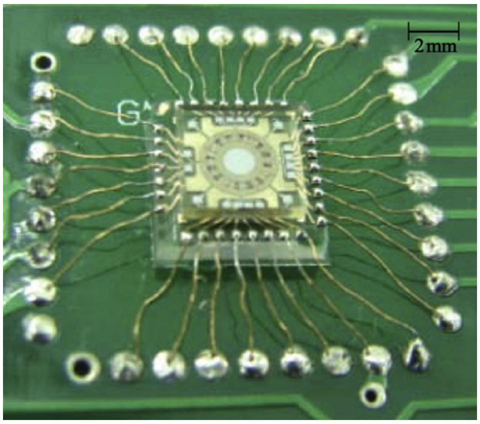

Fig. 1(b). A gyro chip fixed on a printed circuit board.

there are also some state-space or intelligence-control based designs that may be applicable, considerable design efforts are necessarily required and from an engineering viewpoint, practical implementations of these designs are rather complicated [12,13].

In this paper, a compact TITO H_∞ robust controller is designed straightforwardly, which is expected to not only satisfy comprehensive performance requirements of the rebalance loop, but also to be implemented plainly in engineering practice. The outline for the design and verification procedures is as follows. First, in Section 2, a dynamic decoupler matrix is applied to the TITO coupled gyro dynamic model. This decoupler matrix can (1) achieve nominal-case decoupling, (2) define partly steady-state performance requirement, and (3) facilitate the design of the H_∞ robust controller and reduce its potential order. Next, an H_∞ mixed-sensitivity design framework is constructed to handle various specific performance requirements, and a bilinear pole-shifting transform technique is appropriately employed to deal with the ill-conditionness of the decoupled plant. This mixed-sensitivity design is detailed in Section 3. For the synthesized H_∞ robust controller, Section 4 presents thorough frequency-domain analyses and time-domain simulation results under a set of realistic conditions. Finally, Section 5 concludes the paper.

2. Gyro dynamic model and decoupler matrix

2.1. Gyro dynamic model

The dynamic model of the gyro is first introduced as a basis for the following design. In Fig. 2, two main coordinate frames are defined. The $OX_cY_cZ_c$ is the gyro case frame, and the $Oxyz$ is the rotor-referenced frame without spinning, in which the suspended rotor spins around the Oz axis. These two frames coincide with each other if the gyro case is static in the initial space. When external angular rate inputs $\dot{\theta}_x$ and $\dot{\theta}_y$ (with respect to the static inertial space) are applied to the moving vehicle, the instantaneous tilt angles of the rotor μ_x and μ_y with respect to the gyro case occur. Note that instantaneous tilt angles of the rotor with respect to the static inertial space are $\beta_x = \theta_x - \mu_x$ and $\beta_y = \theta_y - \mu_y$, which are omitted in Fig. 2 for clarity.

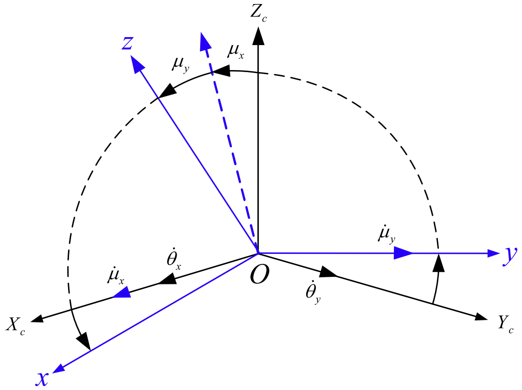

Fig. 2. Orientation of the rotor-referenced frame $Oxyz$ and gyro case frame $OX_cY_cZ_c$.

Table 1
Main geometrical parameters of the rotational MEMS gyro.

Geometry parameter	Value (unit)
Rotor thickness	200 (μm)
Inner size of rotor	731 (μm)
Outer size of rotor	2000 (μm)
Normal radial gap	8 (μm)
Normal axial gap	4 (μm)
Rotor mass	1.537×10^{-5} (kg)
Rotor moment of inertia (about an in-plane axis)	1.76×10^{-11} (kg m^2)

The tilt angles μ_x and μ_y are limited to less than 3×10^{-3} rad by the narrow gaps in the gyro cavity, and then a linearized dynamic model of the gyro can be reasonably derived as [6]

$$\begin{aligned} J\ddot{\mu}_x + H\dot{\mu}_y &= M_x + M_{dx} - J\ddot{\theta}_x - H\dot{\theta}_y \\ J\ddot{\mu}_y - H\dot{\mu}_x &= M_y + M_{dy} - J\ddot{\theta}_y + H\dot{\theta}_x \end{aligned} \tag{1}$$

where, J is the rotor moment of inertia along the in-plane Ox or Oy axis, H represents the Oz axis angular moment of the rotor. $\ddot{\mu}_x$ and $\dot{\mu}_x$ are respectively the second-order and first-order derivatives of μ_x with respect to time, and the same denotations hold true for μ_y, θ_x and θ_y. The M_x and M_y are electrostatic precession torques, and M_{dx} and M_{dy} represent small disturbance torques. Note that in Eq. (1), the viscous damping effect is neglected since the vacuum in the gyro cavity is on the order of 10^{-3} Torr and the mean free path of molecule is significantly larger than the length of the axial or radial cavity gap.

By utilizing the equation $H = 2J\Omega$ with Ω representing a preselected spinning speed of the rotor, Eq. (1) can be simplified into Eq. (2) by means of the Laplace transform. Note that the small disturbance torques M_{dx} and M_{dy} are reasonably neglected.

$$\begin{bmatrix} \mu_x(s) \\ \mu_y(s) \end{bmatrix} = G(s) \begin{bmatrix} M_x(s) \\ M_y(s) \end{bmatrix} - \begin{bmatrix} \theta_x \\ \theta_y \end{bmatrix} \tag{2}$$

with

$$\begin{aligned} G(s) &= \begin{bmatrix} G_{11}(s) & G_{12}(s) \\ G_{21}(s) & G_{22}(s) \end{bmatrix} \\ &= \begin{bmatrix} \dfrac{1/J}{s^2 + (2\Omega)^2} & \dfrac{-2\Omega/J}{s\left[s^2 + (2\Omega)^2\right]} \\ \dfrac{2\Omega/J}{s\left[s^2 + (2\Omega)^2\right]} & \dfrac{1/J}{s^2 + (2\Omega)^2} \end{bmatrix}. \end{aligned} \tag{3}$$